On the Application of the Meshless Local Petrov-Galerkin (MLPG) Method to the Analysis of Shear Deformable Plates

J.Sorić[1], Q. Li[2], T. Jarak[1], S. N. Atluri[2]

Summary

The Meshless Local Petrov-Galerkin (MLPG) approach for the analysis of shear deformable plates is presented. Applying the linear test function in the plate thickness direction, the local symmetric weak form of the equilibrium equations is derived. Discretization is performed by means of the moving least squares (MLS) approximation where the nodal unknown variables are the three fictitious displacement components. The kinematics of three-dimensional solid is adopted. A numerical example illustrates the convergence of numerical results.

Introduction

In recent years, meshless methods have received great attention due to their flexibility in solving boundary value problems. In contrast to the finite element formulations, the meshless computational strategy enables the addition and cancellation of nodes without burdensome remeshing of the entire structure. A variety of meshless methods has been proposed, but most of them are not truly meshless because they require the use of background cells for integration.

The Meshless Local Petrov-Galerkin (MLPG) approach, originally proposed by Atluri and Zhu [1], which requires no elements or background cells in either interpolation or integration is applied in this contribution. The concept of a 3-D solid is adopted for the shear deformable plate analysis, which incorporates the kinematics of a three-dimensional continuum. According to the finite element formulation in [2], the displacement approximations in the thickness and in-plane directions are performed separately. The linear displacement interpolation is performed over the thickness and the moving least squares (MLS) approximation is applied in the in-plane directions. The quadratic polynomial basis and the 6^{th} order spline type weight function are employed. Over the cylindrical local sub-domain, the linear test function in the thickness direction is assumed. The essential boundary conditions are imposed by a penalty method. Due to the linear interpolation of displacements in the thickness direction, some locking phenomena, which will be eliminated in future contributions, may be expected. The performance of the proposed formulation is demonstrated by a numerical example.

[1] Faculty of Mechanical Engineering and Naval Architecture, University of Zagreb, 10000 Zagreb, I. Lučića 5, Croatia

[2] Center for Aerospace Research & Education, University of California, Irvine, Irvine, CA. 92612, USA

Meshless formulation

The Meshless Local Petrov-Galerkin (MLPG) method is applied where the test and trial functions may be chosen from different functional spaces. We start with a local weak form of the 3-D equilibrium equations over a local sub-domain Ω_s, which may be written as

$$\int_{\Omega_s} \left(\sigma_{ij,j} + b_i\right) v_i \mathrm{d}\Omega - \alpha \int_{\Gamma_{su}} (u_i - \bar{u}_i) v_i \mathrm{d}\Gamma = 0\,, \tag{1}$$

where σ_{ij} is the stress tensor and b_i denotes the body force. u_i is the trial function describing the displacement field, while v_i is the test function. The indices i, j which take the values 1,2,3, refer to the Cartesian coordinates x,y,z. Γ_{su} is a part of the boundary $\partial\Omega_s$ of the local sub-domain with the prescribed displacement $\bar{u}_i$, and α denotes a penalty parameter, $\alpha >> 1$. The test functions are assumed as

$$v_i = v_{0i} + z v_{i1}\,, \tag{2}$$

where v_{0i} and v_{1i} are arbitrary constant values, and z is the Cartesian coordinate in the thickness direction of the plate. Using the divergence theorem in (1), inserting (2), and after some suitable rearrangements, the following local symmetric weak form is obtained

$$\begin{aligned} &\left(\int_{L_s} t_i \mathrm{d}\Gamma + \int_{\Gamma_{su}} t_i \mathrm{d}\Gamma + \int_{\Gamma_{st}} \bar{t}_i \mathrm{d}\Gamma + \int_{\Omega_s} b_i \mathrm{d}\Omega - \alpha \int_{\Gamma_{su}} (u_i - \bar{u}_i) \mathrm{d}\Gamma \right) v_{0i} + \\ &\left(\int_{L_s} t_i z \mathrm{d}\Gamma + \int_{\Gamma_{su}} t_i z \mathrm{d}\Gamma + \int_{\Gamma_{st}} \bar{t}_i z \mathrm{d}\Gamma + \int_{\Omega_s} (b_i z - \sigma_{i3}) \mathrm{d}\Omega - \alpha \int_{\Gamma_{su}} (u_i - \bar{u}_i) z \mathrm{d}\Gamma \right) v_{1i} = 0. \end{aligned} \tag{3}$$

Herein the boundary $\partial\Omega_s$ of the local sub-domain is divided in three parts, $\partial\Omega_s = L_s \cup \Gamma_{st} \cup \Gamma_{su}$. L_s is the part of the local boundary inside the global domain, while Γ_{st} and Γ_{su} are the parts of the local boundary which coincide with the global traction boundary and the global geometric boundary, respectively. t_i denotes the components of the surface traction and $\bar{t}_i$ are its prescribed values. Since relation (3) holds for all choices of v_{0i} and v_{1i}, it yields the following expressions

$$\begin{aligned}
&\int_{L_s} t_i \mathrm{d}\Gamma + \int_{\Gamma_{su}} t_i \mathrm{d}\Gamma - \alpha \int_{\Gamma_{su}} u_i \mathrm{d}\Gamma = -\int_{\Gamma_{st}} \bar{t}_i \mathrm{d}\Gamma - \int_{\Omega_s} b_i \mathrm{d}\Omega - \alpha \int_{\Gamma_{su}} \bar{u}_i \mathrm{d}\Gamma \\
&\int_{L_s} t_i z \mathrm{d}\Gamma + \int_{\Gamma_{su}} t_i z \mathrm{d}\Gamma - \int_{\Omega_s} \sigma_{i3} \mathrm{d}\Omega - \alpha \int_{\Gamma_{su}} u_i z \mathrm{d}\Gamma = -\int_{\Gamma_{st}} \bar{t}_i z \mathrm{d}\Gamma - \int_{\Omega_s} b_i z \mathrm{d}\Omega - \alpha \int_{\Gamma_{su}} \bar{u}_i z \mathrm{d}\Gamma,
\end{aligned} \tag{4}$$

which represents a set of six equations for each local sub-domain. If the local sub-domain is entirely within the global domain, all integrals over the boundaries Γ_{st} and Γ_{su} are omitted. Under the assumption of zero body force, the two domain integrations of b_i are also eliminated.

Discretization and Numerical Implementation

The plate is discretized by the nodes on the upper and lower surfaces, as shown in Figure 1. The displacement is described by the components in the local Cartesian coordinate system, $\mathbf{u}^T = \begin{bmatrix} u & v & w \end{bmatrix}$. The linear interpolation is adopted in the thickness direction, while the moving least squares (MLS) approximation is applied in the in-plane directions

$$\mathbf{u} = \sum_{J=1}^{N} \phi_J(x,y) \begin{bmatrix} \left(\frac{1}{2} + \frac{z}{h}\right)\mathbf{I}_3 & \left(\frac{1}{2} - \frac{z}{h}\right)\mathbf{I}_3 \end{bmatrix} \begin{bmatrix} \mathbf{v}_{Ju} \\ \mathbf{v}_{Jl} \end{bmatrix}, \tag{5}$$

where $\phi_J(x,y)$ is the shape function of the MLS approximation [3], while $\mathbf{v}_{Ju}$ and $\mathbf{v}_{Jl}$ are the vectors of the fictitious nodal displacement components on the upper and lower surfaces, respectively. $\mathbf{I}_3$ is the identity matrix 3x3, and h denotes the plate thickness. $2N$ is the total number of nodes in the domain of influence (one value of N is associated with the two nodes through thickness).

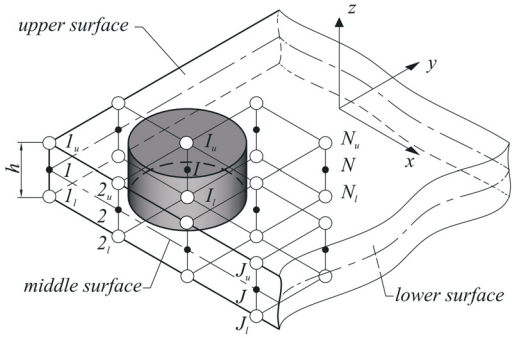

Figure 1. Plate geometry with the local sub-domain

The domain of influence is defined as a region where the weight functions of the nodes within it do not vanish in the local sub-domain of the current nodes. Herein, the shape function is derived by employing the quadratic polynomial basis and the 6th order spline of the weight function.

Equation (5) may be rewritten in the following matrix form as

$$\mathbf{u} = \sum_{J=1}^{N} \mathbf{\Phi}_J \, \mathbf{v}_J \,, \tag{6}$$

where $\mathbf{\Phi}_J = \mathbf{\Phi}_J(x, y, z)$ is the shape function matrix, and $\mathbf{v}_J^T = \left[\mathbf{v}_{Ju} \quad \mathbf{v}_{Jl}\right]$ is the vector of the fictitious nodal values. The 6-dimensional stress vector $\boldsymbol{\sigma}$ and the vector of the surface traction components $\mathbf{t}$ may be expressed according to [4] by the following relations

$$\boldsymbol{\sigma} = \sum_{J=1}^{N} \mathbf{D}\mathbf{B}_J \, \mathbf{v}_J \,, \quad \mathbf{t} = \mathbf{N}\boldsymbol{\sigma} = \sum_{J=1}^{N} \mathbf{N}\mathbf{D}\mathbf{B}_J \, \mathbf{v}_J \,. \tag{7}$$

Herein $\mathbf{B}_J$ is the strain-displacement matrix obtained by the differentiation of the shape functions and $\mathbf{D}$ is the 3-D stress-strain matrix. $\mathbf{N}$ is the matrix describing the outward normal on $\partial\Omega_s$. By means of equations (6) and (7), equations (4) are transformed in the discretized system of linear equations which may be written in the following matrix form

$$\begin{aligned}
&\sum_{J=1}^{N} \left[\int_{L_s} \mathbf{N}\mathbf{D}\mathbf{B}_J \mathrm{d}\Gamma + \int_{\Gamma_{su}} \mathbf{N}\mathbf{D}\mathbf{B}_J \mathrm{d}\Gamma - \alpha \int_{\Gamma_{su}} \mathbf{\Phi}_J \mathrm{d}\Gamma \right] \mathbf{v}_J = -\int_{\Gamma_{st}} \bar{\mathbf{t}} \, \mathrm{d}\Gamma - \int_{\Omega_s} \mathbf{b} \, \mathrm{d}\Omega - \alpha \int_{\Gamma_{su}} \bar{\mathbf{u}} \, \mathrm{d}\Gamma \,, \\
&\sum_{J=1}^{N} \left[\int_{L_s} \mathbf{N}\mathbf{D}\mathbf{B}_J \, z \, \mathrm{d}\Gamma + \int_{\Gamma_{su}} \mathbf{N}\mathbf{D}\mathbf{B}_J \, z \, \mathrm{d}\Gamma - \int_{\Omega_s} \mathbf{D}'\mathbf{B}'_J \, \mathrm{d}\Omega - \alpha \int_{\Gamma_{su}} \mathbf{\Phi}_J \, z \, \mathrm{d}\Gamma \right] \mathbf{v}_J = \\
&\qquad\qquad = -\int_{\Gamma_{st}} \bar{\mathbf{t}} \, z \, \mathrm{d}\Gamma - \int_{\Omega_s} \mathbf{b} \, z \, \mathrm{d}\Omega - \alpha \int_{\Gamma_{su}} \bar{\mathbf{u}} \, z \, \mathrm{d}\Gamma,
\end{aligned} \tag{8}$$

where $\mathbf{D}'$ and $\mathbf{B}'_J$ are the matrices relating to the stress components σ_{i3}. The local sub-domain, where the integration is performed, is chosen as a cylinder surrounding the nodes on the upper and the lower surface, Figure 1. As obvious, we have six unknowns for the two nodes through the thickness. The global set of equations is derived by using a well-known numerical procedure. For a plate with the total number of M nodes placed on the upper and lower surfaces, the set of $6M$ linear algebraic equations with the equal number of unknowns will need to be solved.

Numerical example

As an example, a clamped square plate subjected to uniformly distributed load over the upper surface is considered. The plate thickness to span ratio is $h/a = 0.1$. Due to symmetry, only one quarter of the plate is discretized by the uniformly distributed nodes of 9x9, 11x11, 13x13, 15x15 and 17x17 on the upper and lower surfaces. Computation is performed by using the relations (8) with the omission of body forces. The material data are Young's modulus $E = 10.92 \cdot 10^5$ and Poisson's ratio $\nu = 0$. In that case, using the zero value of Poisson's ratio, the thickness locking due to the linear interpolation over the thickness is avoided. Computations are performed for different values of the weight function circular support radius. It is found that the weight function support significantly affects numerical solutions. Dependency of the plate central deflection on the ratio of the support radius to the radius of local sub-domain for different number of grid points is plotted in Figure 2.

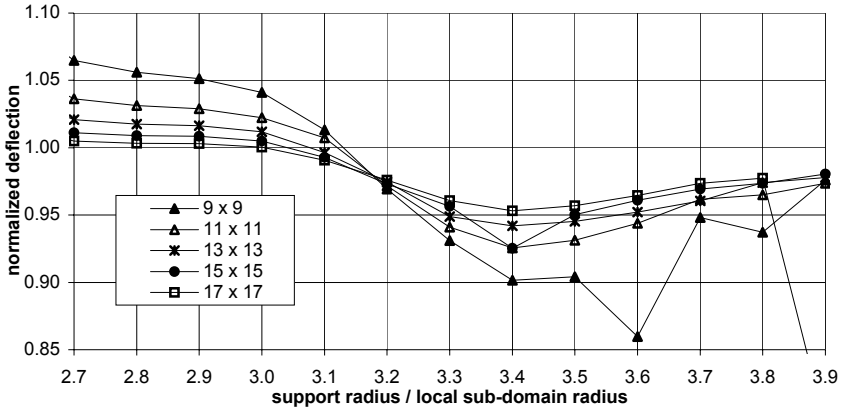

Figure 2 Central deflection of the clamped square plate

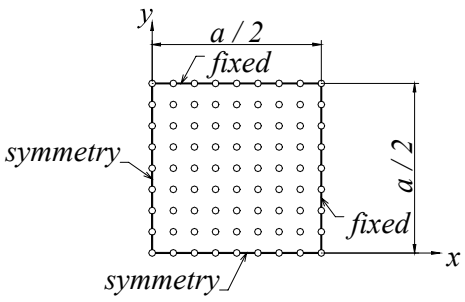

Figure 3 Discretization of one quarter of the square plate surface

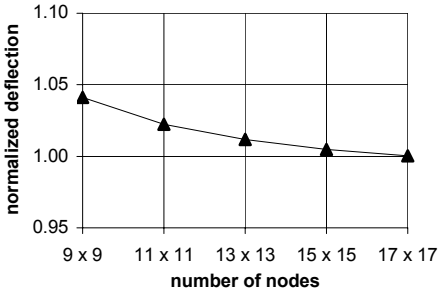

Figure 4 Convergence of the central deflection of the clamped square plate

The deflection is normalized with respect to the exact value. As evident, the noticeable oscillations around the exact value are exhibited. The grid of 9x9 nodes is shown in Figure 3. The convergence to the exact solution with the increase of the grid size is achieved for the ratio of the support radius to the radius of local sub-domain of 3.0. The convergence of the central deflection is plotted in Figure 4.

Conclusion

The Meshless Local Petrov-Galerkin (MLPG) method has been applied to the analysis of shear deformable plates. This numerical method is truly meshless because no elements or background cells are involved in either interpolation or integration. The integration is carried out over the cylindrical local sub-domains. By properly choosing the radius of the circular support of the weight function, a good convergence rate of numerical results is exhibited. Due to the linear interpolation of the displacements in the thickness direction, the thickness locking occurs, which will be eliminated in the future research by using the quadratic interpolation of transversal displacement through the thickness. The proposed formulations will be also extended for the analysis of thin plates, where some remedies to eliminate shear locking phenomena will be adopted.

Acknowledgment

The first author expresses his gratitude to the Fulbright Foundation for the granted financial support by Fulbright scholarship.

Reference

1 Atluri, S. N. and Zhu, T. (1998): "A new meshless local Petrov-Galerkin (MLPG) approach in computational mechanics", *Comput. Mech*., Vol. 22, pp. 117-127.

2 Hauptmann, R. and Schweizerhof, K. (1998): "A systematic development of solid – shell element formulations for linear and non-linear analyses employing only displacement degrees of freedom", *Int. J. Numer. Meth. Engng*,, Vol 42, pp. 49-69.

3 Atluri, S. N. and Shen, S. (2002): *The Meshless Local Petrov-Galerkin (MLPG) Method*, Tech. Science Press.

4 Li, Q., Shen, S., Han, Z.D. and Atluri, S. N. (2003): "Application of Meshless Local Petrov-Galerkin (MLPG) to Problems with Singularities, and Material Discontinuities, in 3-D Elasticity", *CMES: Computer Modeling in Engineering & Sciences,* Vol. 4, pp. 571-585.